



Original article

Design, synthesis and anti-inflammatory evaluation of novel 5-benzylidene-3,4-dihalo-furan-2-one derivatives



Fang Wang, Jun-Rong Sun, Mei-Yan Huang, Hui-Ying Wang, Ping-Hua Sun, Jing Lin, Wei-Min Chen*

Guangdong Province Key Laboratory of Pharmacodynamic Constituents of TCM and New Drugs Research, College of Pharmacy, Jinan University, Huangpu Dadao West, Guangzhou 510632, PR China

ARTICLE INFO

Article history:

Received 9 September 2013
 Received in revised form
 28 October 2013
 Accepted 29 October 2013
 Available online 20 November 2013

Keywords:

3,4-Dihalo-furan-2-one
 Synthesis
 Anti-inflammation
 Action mechanism
 PPAR γ

ABSTRACT

Rosiglitazone has shown promising anti-inflammation effect. To develop preferable anti-inflammatory agents, twenty-two rosiglitazone analogs were synthesized and their anti-inflammatory activity was evaluated. Among these compounds, **6i** and **6k** displayed excellent inhibitory activities on the production of inflammatory mediators, including nitric oxide (NO), tumor necrosis factor- α (TNF- α) and interleukin-6 (IL-6). Furthermore, **6i** and **6k** showed suppression effects on the nuclear factor-kappa B (NF- κ B) and mitogen-activated protein kinase (MAPK) pathways, and this suppression effects could be partially reversed by GW9662, which is a peroxisome proliferator-activated receptor γ (PPAR γ) antagonist. Additionally, our docking results exhibited the well combination of **6i** and **6k** to PPAR γ . So the anti-inflammation activity of **6i** and **6k** was due at least in part, to their interaction with PPAR γ .

© 2013 Elsevier Masson SAS. All rights reserved.

1. Introduction

Inflammation is a fundamental protective response of the immune system to pathogens or harmful irritants and the classical signs of inflammation are redness, swelling, heat, and pain [1,2]. Paradoxically, the inflammatory process itself may cause tissue damage and lead to a host of diseases while it is a fundamental protective response. For example, excessive production of inflammatory mediators, such as nitric oxide (NO), interleukin-6 (IL-6) and tumor necrosis factor- α (TNF- α) [3–5], as well as aberrant activation of nuclear factor-kappa B (NF- κ B) and mitogen-activated protein kinase (MAPK) pathways may be observed after infection or injury, which have been implicated in many inflammatory diseases [6,7].

Recently, accumulating evidences have illustrated that peroxisome proliferator-activated receptor γ (PPAR γ), which is originally known as a nuclear receptor and functions as transcription factor, has emerged as a potential target for the treatment of inflammatory diseases such as ulcerative colitis, atherosclerosis, asthma and rheumatoid arthritis [8–12]. It is well known that the PPAR γ agonists-thiazolidinediones (TZDs), such as rosiglitazone

and pioglitazone, are capable of reducing the expression of inflammatory genes in macrophages [12,13]. In particular, rosiglitazone has reported to have promising anti-inflammatory effect through the mechanisms that inhibition of TNF- α and IL-6 production, as well as activation of PPAR γ receptor and inhibition the NF- κ B activation [14–17]. Thus to develop small molecules to activate PPAR γ , thereby inhibiting the production of inflammatory mediators, as well as suppressing activation of NF- κ B and MAPK cascades has been shown to be a feasible anti-inflammation strategy.

In order to develop novel agents that are preferable in anti-inflammation, at here, a variety of structural modifications of the rosiglitazone have been carried out. Based on the result of our previous work that compounds bearing a halogenated furanone moiety had excellent anti-bacterial activity, as well as the fact that bacterial infection is an important factor for inflammation, we hypothesized that using halogenated furanones to transform rosiglitazone's skeleton may lead to more active compounds [18–20]. In this regard, according to the bioisosterism, a series of rosiglitazone analogs with the thiazolidinedione moiety replaced by halogenated furanone were designed, synthesized, and their anti-inflammation activities were examined with regard to their effects on the production of inflammatory mediators, including NO, TNF- α and IL-6 in lipopolysaccharide (LPS)-stimulated RAW264.7 cells. Moreover, western blot experiments and docking studies were performed in

* Corresponding author. Tel.: +86 20 8522 4497; fax: +86 20 8522 4766.
 E-mail address: twmchen@jnu.edu.cn (W.-M. Chen).

an attempt to illustrate the anti-inflammation mechanism of **6i** and **6k**, which were two compounds with dramatically improved anti-inflammatory activity.

2. Chemistry

In order to develop preferable anti-inflammatory agents, a variety of structural modifications of the rosiglitazone have been carried out according to the bioisosterism. As shown in [Scheme 1](#), the modifications include: (a) replaced the thiazolidinedione moiety ([Scheme 1](#): section A) of rosiglitazone with halogenated furanone, which was an important structure that could improve the drug activity because of the role inhibition of bacteria [18–20]; (b) introduction of electron-donating substituent (methoxyl or ethoxy) into the benzene ring ([Scheme 1](#): section B); (c) replayed the section C ([Scheme 1](#)) with pyridyl group or tetramethylpyrazinyl group which showed PPAR γ agonist and anti-inflammatory activity [21,22].

The synthesis of the designed compounds in [Scheme 1](#) was accomplished as outlined in [Scheme 2](#) (**6a–6w**) and [Scheme 3](#) (**7a–7d**).

In brief, mucochloric acid or mucobromic acid as starting materials, were converted into halogenated furanones via a reaction employed sodium borohydride as reducing agent and concentrated sulfuric acid as dehydrating agent in absolute methanol [23,24]. The halogenated furanones then reacted with hydroxyl benzaldehydes to yield 3,4-dihalo-5-(4-hydroxybenzylidene) furan-2(5H)-one intermediates via Knoevenagel reaction [24,25]. This condensation was carried out in refluxing toluene, containing a catalytic amount of piperidinium acetate. Finally the 3,4-dihalo-5-(4-hydroxybenzylidene)furan-2(5H)-ones were connected to form ether with (3,5,6-trimethylpyrazin-2-yl)methanol (TMP-OH) or pyridine derivatives via Mitsunobu coupling [26,27] to produce end-products with a yield of 70–80% (as shown in [Scheme 2](#)). Besides, 5-benzylidenethiazolidine-2,4-dione derivatives were synthesized from 2,3,5,6-tetramethylpyrazine (TMP) and *N*-bromosuccinimide (NBS) via free radical reaction [28]. The typical subsequent synthetic procedure involved the combination of 2-(bromomethyl)-3,5,6-trimethylpyrazine (TMP-Br) and hydroxyl benzaldehyde derivatives through the formation of ether bonds

under alkaline condition [29]. The latter compounds and thiazolidine-2,4-dione were dissolved in anhydrous toluene and refluxed for 2 h under nitrogen to give four compounds (as shown in [Scheme 3](#)).

There was a problem that *E* and *Z* geometrical isomers around the exocyclic double bond (CH=C) were possible for **6a–6w** and **7a–7d**. ^1H NMR spectrum of the twenty-two compounds showed only one signal for the benzyl fork proton that the chemical shifts were basically in the same range from 6.33 to 6.40 ppm and from 7.70 to 7.78 ppm for **6a–6w** (in deuterated chloroform solution) and **7a–7d** (in deuterated dimethylsulfoxide solution), respectively. Additionally, the *Z*-configuration had been reported thermodynamically more stable than the *E*-configuration [30,31]. Our results as well as the judgment of similar compounds in the literatures [32,33] suggested that the configuration of synthesized compounds was single *Z* configuration.

All the compounds were fully analyzed and characterized by ^1H , ^{13}C nuclear magnetic resonance (NMR), mass spectrometry (MS) and high resolution mass spectrometry (HRMS) before entering the biological evaluation.

3. Results and discussion

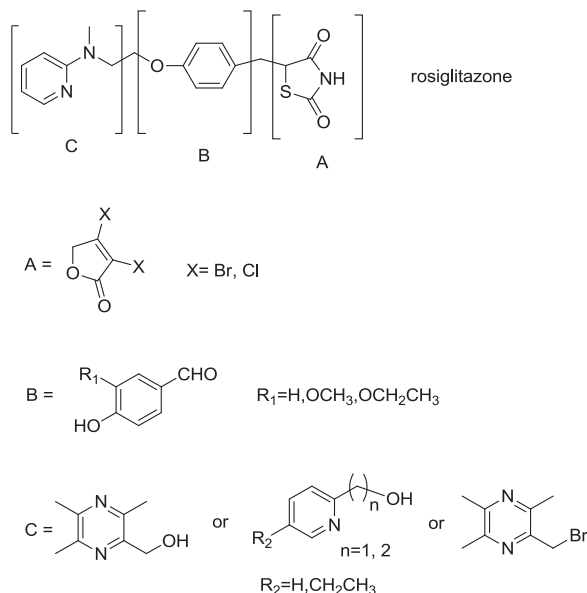
3.1. Inhibition of NO production in (LPS)-stimulated RAW264.7 cells

Nitric oxide (NO) is a significant pro-inflammatory mediator. Excessive production of NO was found to be associated with the pathogenesis of inflammation diseases, and it is generally accepted that NO inhibitors may offer potential opportunity to identify new therapeutic method for the inflammatory diseases [34]. So first all the synthesized compounds were investigated for their inhibitory activity against lipopolysaccharide (LPS)-induced NO release in RAW264.7 cells (As shown in Fig. S1, LPS treatment caused significant changes in cell morphologies, which indicated that inflammation could be induced by LPS). Here rosiglitazone and indomethacin ([Fig. 1](#)) were chosen as positive controls. As depicted in [Table 1](#), most of the 5-benzylidene-3,4-dihalo-furan-2-one derivatives (**6a–6w**) displayed improved NO inhibitory activity compared to rosiglitazone and indomethacin. In particular, two compounds (**6i** and **6k**) exhibited excellent activity, and their NO inhibition rates exceeded 75% at the concentration of 10 μM . Another four 5-benzylidenethiazolidine-2,4-dione derivatives (**7a–7d**) with TMP substituted were slightly less active.

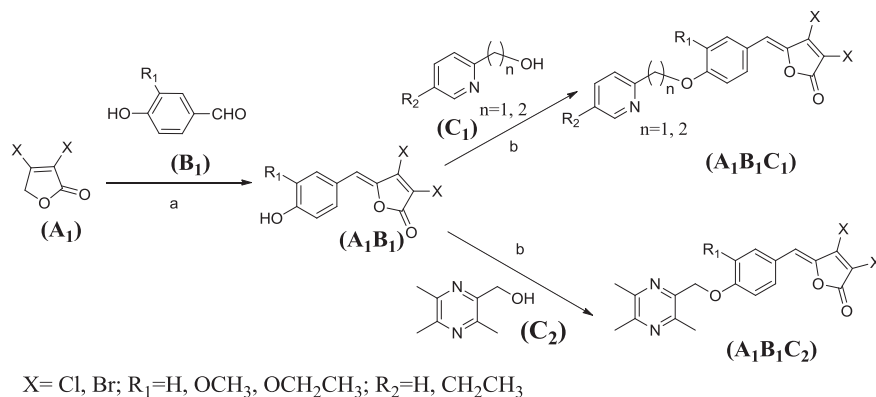
Based on these results, some preliminary structure–activity relationship (SAR) of the rosiglitazone analogs could be summarized: (a) 3,4-dihalo-furan-2-one structure was conducive to anti-inflammatory activity (**6a–6w** compared to **7a–7d**, such as **6w** compared to **7b**); (b) a two-atom linker between the ring B and ring C ([Scheme 2](#)) would be favorable (**6h** compared to **6n**); (c) electron-donating substituent (methoxyl or ethoxyl) at phenyl ring would increase its NO inhibitory activity (**6h** and **6j** compared to **6a**); (d) TMP substitution almost had no effect on the anti-inflammatory activity (**6v** compared to **6b**). These results will be really useful in the future to guide the design and modification of new candidate anti-inflammatory agents.

3.2. Cytotoxicity in RAW264.7 cells

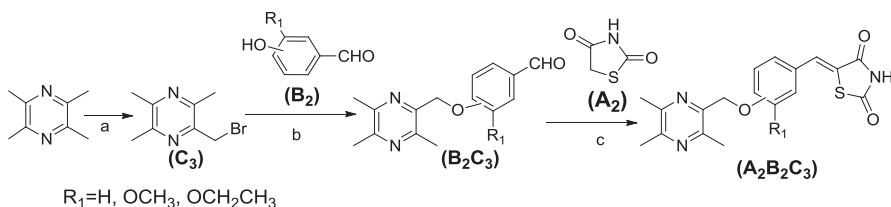
To investigate whether the NO inhibitory activities of **6i** and **6k** were related to cell viability, their cytotoxicities in RAW264.7 cells were examined by methyl thiazolyl tetrazolium (MTT) assay. As shown in [Table 2](#), all the agents (rosiglitazone, indomethacin, **6i**, **6k**, GW9662 and LPS) at the concentrations we detected here had no obviously cytotoxicity in RAW264.7 cells, and the relative cell



Scheme 1. Design strategy for rosiglitazone analogs.



Scheme 2. General synthesis of compounds **6a–6w**. Reagents and conditions: (a) 2-methyl piperidine, CH₃COOH, toluene, 2 h; (b) PPh₃, DEAD, THF, 24 h.



Scheme 3. General synthesis of compounds **7a–7d**. Reagents and conditions: (a) NBS, (PhCO)₂O₂, CCl₄, 12 h; (b) K₂CO₃, DMF, 10 h; (c) 2-methyl piperidine, CH₃COOH, toluene, 2 h.

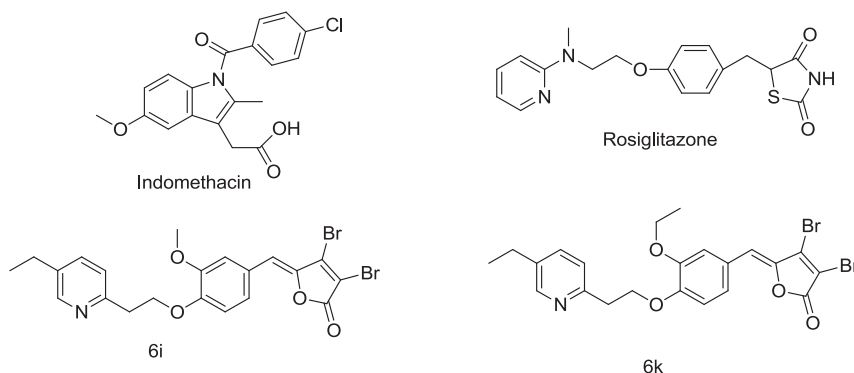


Fig. 1. Chemical structures of indomethacin, rosiglitazone, **6i** and **6k**.

viabilities of the treated cells were all more than 90%. These results indicated that the NO inhibitory effects of **6i** and **6k** were likely to be attributed to the interaction of these two compounds and their specific target. These non-toxic concentrations were further used in subsequent experiment processes.

3.3. Inhibition of TNF- α and IL-6 production in RAW264.7 cells

TNF- α and IL-6 are two crucial pro-inflammatory cytokines which are of paramount importance in inflammatory diseases, and widely recognized that inhibition of their generations would be an effective method for treatment of inflammation [35]. So next, the inhibitory effects of **6i** and **6k** on TNF- α and IL-6 production were investigated. Rosiglitazone and indomethacin (Fig. 1) were also used as positive reference drugs. The effects of these four compounds were evaluated using a fixed concentration of 10 μ M and in a time-dependent manner.

The results (Table 3) showed that the LPS-induced production of TNF- α and IL-6 were significantly decreased by **6i** and **6k**

treatment, and their inhibitory effects were evidently better than that of the positive control drugs treatment on both TNF- α and IL-6 production at all three detection time. Noticeably, **6k** exhibited significant improvement in inhibition of IL-6 production compared to control drugs. All the above results suggested that **6i**, especially **6k**, were excellent agents in anti-inflammation effect. Next, a plenty of efforts were performed to explore the possible anti-inflammatory mechanism of **6i** and **6k**.

3.4. Western blot for interpreting possible mechanism

It has been reported that NF- κ B and MAPK activation (phosphorylation) was quite significant in the regulation of inflammation because of their crucial roles in the mediation of the production of NO, TNF- α , IL-6, and other inflammatory mediators in activated macrophages [36–40]. And it is well accepted that the up-regulation of the synthesis of inflammatory mediators induced by LPS, derived involved NF- κ B and MAPK activation, was modulated by PPAR γ , and the MAPK and NF- κ B activation could be inhibited by

Table 1

The inhibitory effects of the synthesized compounds on NO production in LPS-stimulated RAW264.7 cells.

Compounds	NO inhibition (%) ^a	Compounds	NO inhibition (%) ^a
Rosi ^b	16.7 ± 3.9**	6p	40.8 ± 5.1*
Indo ^c	31.3 ± 2.9**	6q	16.3 ± 3.4*
6a	38.0 ± 6.7*	6r	50.4 ± 2.6*
6b	29.2 ± 9.5*	6s	36.8 ± 3.2*
6c	43.6 ± 2.8**	6t	38.9 ± 5.9*
6g	20.2 ± 6.1*	6u	36.4 ± 1.7**
6h	54.7 ± 2.3**	6v	30.1 ± 2.4**
6i	75.8 ± 4.3*	6w	37.2 ± 7.1*
6j	62.9 ± 6.8*	7a	19.3 ± 8.0*
6k	80.1 ± 4.1*	7b	24.9 ± 6.1*
6l	42.2 ± 3.7*	7c	30.7 ± 4.9*
6n	33.9 ± 4.7*	7d	23.5 ± 2.2**

***P* < 0.01, **P* < 0.05 versus the LPS (treated with LPS only) group.

^a Results were showed as means ± SD (*n* = 4) of at least three independent experiments.

^b Rosi: rosiglitazone.

^c Indo: indomethacin.

Table 2

Effects of compounds on the viability of RAW264.7 cells.

Compounds	Concentrations	Cell viability (%) ^a
Blank		100.0 ± 5.8**
Rosi ^b	10 μM	99.7 ± 6.9*
Indo ^c	10 μM	100.8 ± 7.4*
6i	10 μM	98.1 ± 7.2*
6k	10 μM	93.1 ± 5.6**
GW9662	5 μM	101.0 ± 6.3*
LPS	500 ng/mL	99.4 ± 4.7**
LPS	100 ng/mL	103.6 ± 3.0**

***P* < 0.01, **P* < 0.05 compared to the blank (cultured with fresh medium only) group.

^a Results were expressed as means ± SD (*n* = 5) of three independent experiments.

^b Rosi: rosiglitazone.

^c Indo: indomethacin.

pre-treatment with PPAR γ agonists, such as rosiglitazone [41]. Therefore, in this study, western blot analysis was employed to investigate whether the anti-inflammatory effects of **6i** and **6k** were associated with the PPAR γ mediated activation of NF- κ B and MAPK. The proteins we detected here included two NF- κ B pathway proteins: NF- κ B p65 and inhibitor kappa B alpha (I κ B α) kinase [42–44], as well as three MAPK cascades: extracellular regulated protein kinases (ERK1/2, or p42/44), c-Jun N-terminal kinases (JNK) and p38 MAPK [45–47].

As shown in Fig. 2, LPS significantly increased the levels of phosphorylated NF- κ B p65, I κ B α , JNK, ERK1/2 and p38 MAPK, and both **6i** and **6k** treatment could lead to a decrease in activating of these proteins in varying degrees. Furthermore, the phosphorylations of NF- κ B p65, I κ B α , ERK1/2 and p38 MAPK were obviously inhibited after treatment with **6i** and **6k**, while they had slightly antagonized effect on phosphorylation of I κ B α . Moreover, **6k** significantly inhibited the phosphorylation of JNK. Additionally, it was worth to notice that the suppressive effects of **6i** and **6k** on the protein phosphorylations could be reversed by GW9662 (5 μM), which is a highly selective and irreversible PPAR γ antagonist [48]. Combination of all the western blot results, we hypothesized that anti-inflammation effects of **6i** and **6k** were due to at least in part, to their interaction with PPAR γ , thereby suppressing activation of NF- κ B and MAPK cascades, resulting in decreased NO, TNF- α and IL-6 levels. Nonetheless, further studies were needed to confirm this hypothesis.

3.5. Docking analysis

To confirm the above hypothesis that **6i** and **6k** were likely to act as PPAR γ agonist, we performed some docking analysis to investigate the interaction of **6i** and **6k** with PPAR γ . For the docking studies, rosiglitazone and indomethacin, which are two identified PPAR γ agonists, were used as reference molecules. The structure of PPAR γ used in the docking studies was obtained from the Protein Data Bank (PDB ID: 2PRG) and all docking experiments were performed using SYBYL 8.1 program package of Tripos [49]. The docking scores of all four molecules with PPAR γ were shown in Table 4.

In line with the western blot results, **6i** and **6k** could well interact with PPAR γ , even with higher docking scores than that for rosiglitazone and indomethacin, which implied the possibility of the directly interaction of **6i** and **6k** with PPAR γ . Furthermore, the MOLCAD (Molecular Computer Aided Design) Multi-Channel surfaces structures displayed with cavity depth potential or hydrogen bonds of the PPAR γ -binding site within the four compounds were also developed to explore the ligand–receptor interaction details. Fig. 3 depicted the MOLCAD cavity depth potential surface of the PPAR γ pocket within four compounds, the cavity depth color ramp ranged from blue (low depth values = outside of the pocket) to orange (high depth values = deep inside the pocket). Fig. 4 displayed the hydrogen bonds formed between PPAR γ and four compounds, the hydrogen bonds were showed as yellow dashed lines.

As shown in Fig. 3, four ligands were able to bind to PPAR γ while with different depths. Rosiglitazone and indomethacin were stayed in a blue region which indicated a relative low depth, while compounds **6i** and **6k** were oriented in a light yellow region which demonstrated that the majority parts of these two molecules were anchored deep inside the pocket. And as shown in Fig. 4, several hydrogen bonds formed between **6i**, **6k** and PPAR γ . In summary, our docking results exhibited the strong binding ability of **6i** and **6k** to PPAR γ , which provided strong evidence for the hypothesis that PPAR γ was, at least one of the specific targets of **6i** and **6k**.

4. Conclusions

In this study, a series of novel 5-benzylidene-3,4-dihalo-furan-2-one derivatives, obtained from the structural modifications of the

Table 3

The inhibitory effects of rosiglitazone, indomethacin, **6i** and **6k** on LPS-induced TNF- α and IL-6 production in RAW264.7 cells.

Compounds	TNF- α (pg/mL) ^a		
	6 h	12 h	24 h
Blank	5.9 ± 0.5	11.8 ± 1.2	38.3 ± 3.3
LPS	455.4 ± 41.1**	661.7 ± 59.4**	1474.0 ± 65.7*
LPS + Rosi ^b	416.9 ± 19.7**	631.3 ± 68.0*	1293.8 ± 94.9*
LPS + Indo ^c	366.5 ± 55.1*	612.6 ± 54.6*	1242.0 ± 80.3**
LPS+ 6i	347.1 ± 35.8**	575.6 ± 39.6*	1110.5 ± 84.5*
LPS+ 6k	323.8 ± 46.3*	519.8 ± 42.1**	1044.2 ± 132.8*
Compounds	IL-6 (pg/mL) ^a		
	6 h	12 h	24 h
Blank	7.2 ± 0.9	13.9 ± 2.6	45.1 ± 5.6
LPS	3065.4 ± 166.4**	4014.2 ± 244.8*	9546.6 ± 595.0*
LPS + Rosi ^b	2783.9 ± 136.1**	3477.9 ± 145.9**	8388.6 ± 446.9*
LPS + Indo ^c	2313.5 ± 218.0*	2989.6 ± 228.9*	7645.9 ± 369.1**
LPS + 6i	1705.9 ± 124.1**	2528.4 ± 170.2*	6360.0 ± 635.5*
LPS + 6k	598.1 ± 117.1**	902.2 ± 137.8**	2360.2 ± 482.1*

***P* < 0.01, **P* < 0.05 versus the LPS (treated with LPS only) group.

^a Results were showed as means ± SD (*n* = 3) of three independent experiments.

^b Rosi: rosiglitazone.

^c Indo: indomethacin.

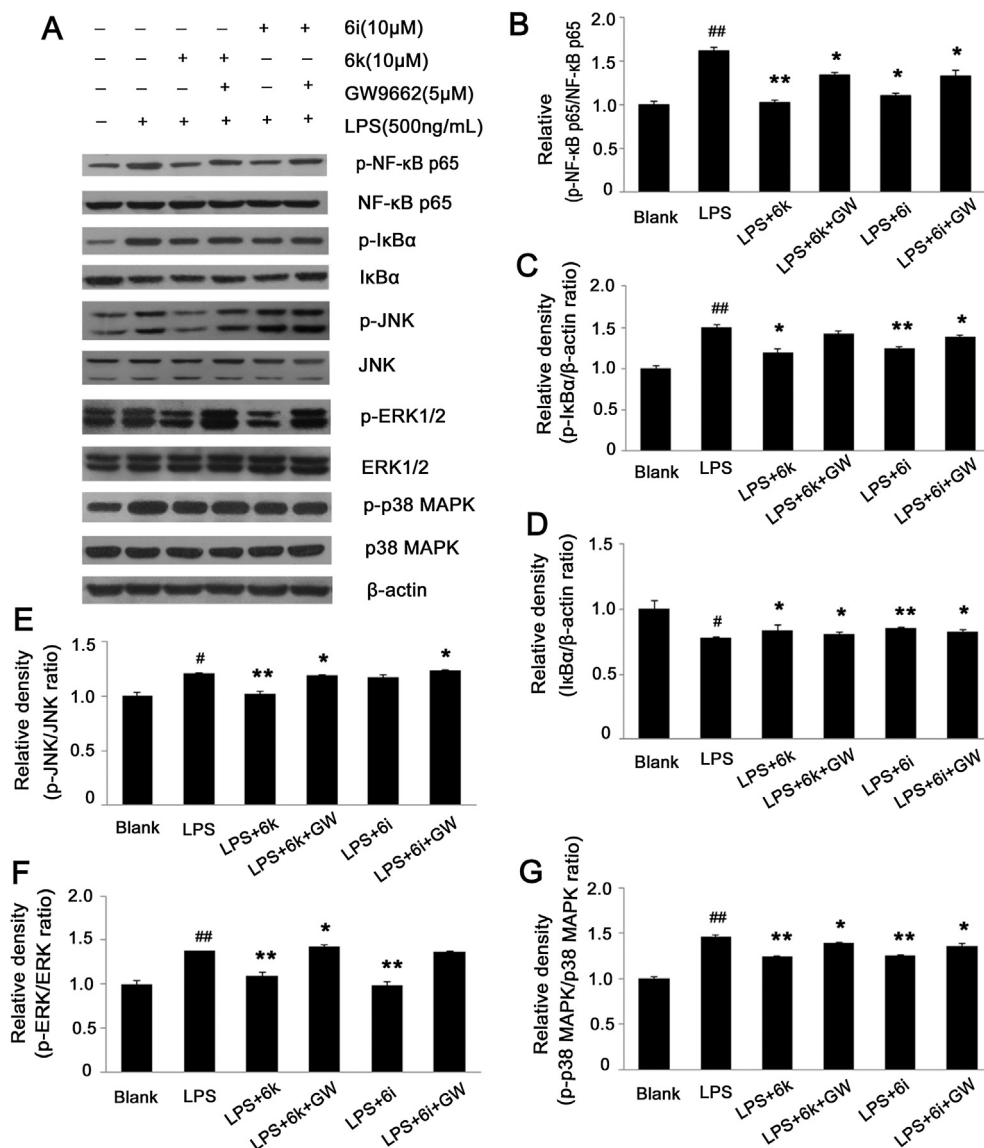


Fig. 2. The effects of compounds **6i** and **6k** on the LPS-induced phosphorylation of NF-κB p65, IκBα, JNK, ERK1/2 and p38 MAPK in RAW264.7 cells. RAW264.7 cells were treated with **6i** (10 μM), **6k** (10 μM), GW9662 (5 μM), and LPS (500 ng/mL) for 4 h. The levels of NF-κB p65, IκBα, JNK, ERK1/2, and p38 MAPK proteins, and their phosphorylated forms were analyzed using western blotting. Data were presented as means ± SD ($n = 3$). ^{##} $P < 0.01$, [#] $P < 0.05$ versus the blank (cultured with fresh medium only) group; ^{**} $P < 0.01$, ^{*} $P < 0.05$ versus the LPS (treated with LPS only) group.

PPAR γ agonist-rosiglitazone, were synthesized and their bioactivities were evaluated. Among these compounds, two promising compounds (**6i** and **6k**) for the treatment of inflammatory diseases were identified. Mechanism studies revealed that, like rosiglitazone, anti-inflammation activity of **6i** and **6k** was due at least in part, to their interaction with PPAR γ , thereby suppressing activation of NF-κB and MAPK cascades, resulting in decreased NO, TNF- α and IL-6 levels. These results further confirmed the previous proposal that PPAR γ might be a feasible anti-inflammatory target. Moreover, SAR analysis illustrated that compounds with the

halogenated furanone structure, which was an important structure of some bacterial inhibitors, generally exhibited improved anti-inflammation activity compared to PPAR γ agonist-rosiglitazone, which suggested that combination of the structural features with anti-bacterial activity into the potential PPAR γ agonists to obtain molecules with both anti-bacterial and PPAR γ activation properties would be an effective strategy to develop preferable anti-inflammatory agents.

5. Experimental section

5.1. Chemistry

5.1.1. General procedure for synthesis of halogenated furanone derivatives (**A1**)

The 3,4-dihalo-furan-2(5H)-ones (**A1**) were prepared according to our previously reported methods [29].

Table 4

Docking scores for the combination of rosiglitazone, indomethacin, **6i** and **6k** to PPAR γ .

Compounds	Rosi	Indo	6i	6k
Scores	6.94	4.92	8.07	8.52

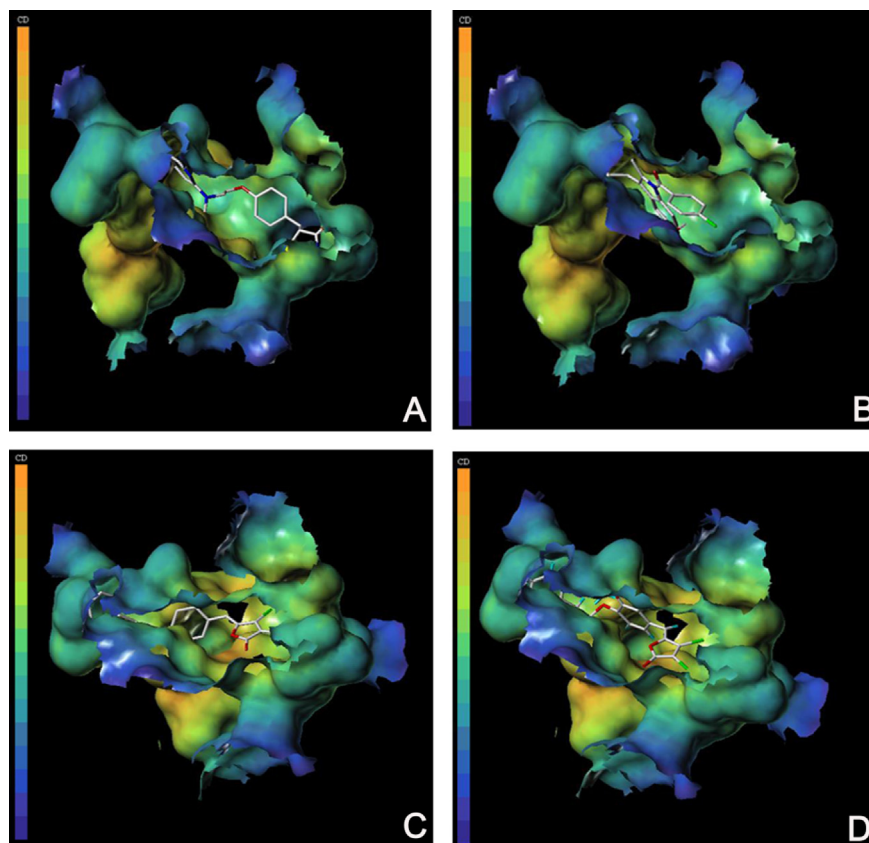


Fig. 3. The MOLCAD Multi-Channel surface structures displayed with cavity depth of the PPAR γ within the (A) rosiglitazone, (B) indomethacin, (C) **6i** and (D) **6k**. The color ramp for cavity depth ranged from blue (outside of the pocket; most negative) to orange (deep inside the pocket; most positive). (For interpretation of the references to color in this figure legend, the reader is referred to the web version of this article.)

5.1.2. General procedure for synthesis of 3,4-dihalo-5-(4-hydroxybenzylidene)furan-2(5H)-one intermediates (**A1B1**)

Benzaldehyde derivatives (**B1**, 1.0 mmol) and halogenated furanones (**A1**, 1.0 mmol) were dissolved in anhydrous toluene (30 mL), and then a catalytic amount of 2-methyl piperidine and glacial acetic acid were slowly dropped to the solution under the atmosphere of nitrogen. The reaction mixture was refluxed at 130 °C for 2 h until the disappearance of starting materials (TLC analysis), and then cooled to room temperature. The toluene was removed under reduced pressure and the residue was dissolved in methanol. This solution was concentrated and purified by silica gel column chromatography with ethyl acetate-petroleum (1:12) as eluent to produce resultant intermediates.

5.1.2.1. 3,4-Dibromo-5-(4-hydroxybenzylidene)furan-2(5H)-one (Z:E = 92:8). Yellow solid; yield 35.7%. $^1\text{H NMR}$ (300 MHz, DMSO- d_6) Z type δ 10.28 (s, 1H), 7.72 (d, $J = 8.7$ Hz, 2.07H), 6.86 (d, $J = 8.7$ Hz, 2.06H), 6.57 (s, 0.99H); E type δ 10.28 (s, 1H), 7.35 (d, $J = 8.8$ Hz, 0.10H), 7.16 (s, 0.09H), 6.81 (d, $J = 8.8$ Hz, 0.12H). $^{13}\text{C NMR}$ (75 MHz, DMSO- d_6) δ 163.9, 160.1, 143.9, 138.0, 133.5, 123.6, 116.7, 114.6, 111.3. ESI-MS m/z : 345.2 [M - H] $^-$.

5.1.2.2. 3,4-Dichloro-5-(4-hydroxybenzylidene)furan-2(5H)-one (Z:E = 92:8). Yellow solid; yield 37.3%. $^1\text{H NMR}$ (300 MHz, DMSO- d_6) Z type δ 10.27 (s, 1H), 7.71 (d, $J = 8.7$ Hz, 1.98H), 6.88 (d, $J = 8.7$ Hz, 1.96H), 6.62 (s, 0.97H); E type δ 10.27 (s, 1H), 7.40 (d, $J = 9.0$ Hz, 0.10H), 7.31 (s, 0.08H), 6.82 (d, $J = 9.0$ Hz, 0.12H). $^{13}\text{C NMR}$ (75 MHz, DMSO- d_6) δ 162.6, 160.1, 142.5, 141.3, 133.6, 123.3, 117.2, 116.7, 113.4. ESI-MS m/z : 255.2 [M - H] $^-$.

$^1\text{H NMR}$ (75 MHz, DMSO- d_6) δ 162.6, 160.1, 142.5, 141.3, 133.6, 123.3, 117.2, 116.7, 113.4. ESI-MS m/z : 255.2 [M - H] $^-$.

5.1.2.3. (Z)-3,4-Dibromo-5-(4-hydroxy-3-methoxybenzylidene)furan-2(5H)-one. Yellow solid; yield 33.0%. $^1\text{H NMR}$ (300 MHz, DMSO- d_6) δ 9.88 (s, 1H), 7.44 (s, 1H), 7.39 (d, $J = 1.8$ Hz, 1H), 6.87 (d, $J = 1.8$ Hz, 1H), 6.58 (s, 1H), 3.81 (s, 3H). $^{13}\text{C NMR}$ (75 MHz, DMSO- d_6) δ 163.9, 149.8, 148.2, 144.0, 138.0, 125.8, 123.9, 116.6, 115.2, 114.9, 111.2, 56.1. ESI-MS m/z : 375.4 [M - H] $^-$.

5.1.2.4. (Z)-3,4-Dichloro-5-(4-hydroxy-3-methoxybenzylidene)furan-2(5H)-one. Yellow solid; yield 36.1%. $^1\text{H NMR}$ (300 MHz, DMSO- d_6) δ 9.91 (s, 1H), 7.41 (d, $J = 1.8$ Hz, 1H), 7.37 (d, $J = 1.8$ Hz, 1H), 6.90 (d, 1H), 6.62 (s, 1H), 3.81 (s, 3H). $^{13}\text{C NMR}$ (75 MHz, DMSO- d_6) δ 162.5, 149.8, 148.3, 142.5, 141.4, 126.0, 123.7, 117.2, 116.6, 115.2, 113.7, 56.1. ESI-MS m/z : 285.3 [M - H] $^-$.

5.1.2.5. (Z)-3,4-Dibromo-5-(3-ethoxy-4-hydroxybenzylidene)furan-2(5H)-one. Red solid; yield 30.1%. $^1\text{H NMR}$ (300 MHz, DMSO- d_6) δ 9.83 (s, 1H), 7.44 (s, 1H), 7.40 (d, $J = 1.8$ Hz, 1H), 6.90 (d, $J = 1.8$ Hz, 1H), 6.58 (s, 1H), 4.08 (q, $J = 7.2$ Hz, 2H), 1.36 (t, $J = 7.2$ Hz, 3H). $^{13}\text{C NMR}$ (75 MHz, DMSO- d_6) δ 163.9, 150.0, 147.4, 144.0, 138.0, 125.9, 124.0, 116.7, 116.4, 114.9, 111.2, 64.4, 15.1. ESI-MS m/z : 389.4 [M - H] $^-$.

5.1.2.6. (Z)-3,4-Dichloro-5-(3-ethoxy-4-hydroxybenzylidene)furan-2(5H)-one. Red solid; yield 37.1%. $^1\text{H NMR}$ (300 MHz, DMSO- d_6) δ 9.83 (s, 1H), 7.40 (d, $J = 1.8$ Hz, 1H), 7.35 (d, $J = 1.8$ Hz, 1H), 6.90

5.1.4.5. (*Z*)-3,4-Dibromo-5-(3-methoxy-4-(2-(pyridin-2-yl)ethoxy)benzylidene)furan-2(5*H*)-one (**6h**). Yellow solid; yield 71.1%. ¹H NMR (300 MHz, CDCl₃) δ 8.56 (d, *J* = 4.5 Hz, 1H), 7.68 (td, *J* = 7.5, 1.5 Hz, 1H), 7.41 (d, *J* = 1.8 Hz, 1H), 7.35 (d, *J* = 7.5 Hz, 1H), 7.29 (dd, *J* = 8.4, 1.8 Hz, 1H), 7.21 (dd, *J* = 4.5, 1.5 Hz, 1H), 6.93 (d, *J* = 8.4 Hz, 1H), 6.36 (s, 1H), 4.48 (t, *J* = 6.9 Hz, 2H), 3.9 (s, 3H), 3.38 (t, *J* = 6.9 Hz, 2H). ¹³C NMR (75 MHz, CDCl₃) δ 163.5, 160.3, 157.5, 150.3, 149.5, 148.5, 144.3, 137.3, 125.8, 125.2, 124.3, 122.0, 114.5, 113.5, 112.9, 111.6, 68.1, 56.1, 37.4. ESI-MS *m/z*: 480.2 [M + H]⁺. HRMS (ESI) *m/z*: 479.9435 [M + H]⁺; Calcd for C₁₉H₁₅Br₂NO₄ (M + H) 479.9447.

5.1.4.6. (*Z*)-3,4-Dibromo-5-(4-(2-(5-ethylpyridin-2-yl)ethoxy)-3-methoxybenzylidene) furan-2(5*H*)-one (**6i**). Yellow solid; yield 81.3%. ¹H NMR (300 MHz, CDCl₃) δ 8.39 (s, 1H), 7.47 (d, *J* = 7.9 Hz, 1H), 7.42 (d, *J* = 2.1 Hz, 1H), 7.30 (dd, *J* = 8.4, 2.1 Hz, 1H), 7.22 (d, *J* = 7.9 Hz, 1H), 6.94 (d, *J* = 8.4 Hz, 1H), 6.38 (s, 1H), 4.46 (t, *J* = 7.1 Hz, 2H), 3.90 (s, 3H), 3.32 (t, *J* = 7.1 Hz, 2H), 2.64 (q, *J* = 7.6 Hz, 2H), 1.25 (t, *J* = 7.6 Hz, 3H). ¹³C NMR (75 MHz, CDCl₃) δ 163.5, 155.1, 150.5, 149.5, 148.8, 144.2, 137.3, 137.2, 136.0, 125.7, 125.0, 123.5, 114.5, 113.5, 112.8, 111.5, 68.3, 56.1, 37.2, 25.7, 15.3. ESI-MS *m/z*: 508.3 [M + H]⁺. HRMS (ESI) *m/z*: 507.9752 [M + H]⁺; Calcd for C₂₁H₁₉Br₂NO₄ (M + H) 507.9760.

5.1.4.7. (*Z*)-3,4-Dibromo-5-(3-ethoxy-4-(2-(pyridin-2-yl)ethoxy)benzylidene)furan-2(5*H*)-one (**6j**). Yellow solid; yield 76.3%. ¹H NMR (300 MHz, CDCl₃) δ 8.55 (d, *J* = 4.8 Hz, 1H), 7.63 (td, *J* = 7.7, 1.8 Hz, 1H), 7.41 (d, *J* = 2.1 Hz, 1H), 7.34 (d, *J* = 7.7 Hz, 1H), 7.32–7.27 (m, 1H), 7.16 (dd, *J* = 4.8, 1.8 Hz, 1H), 6.93 (d, *J* = 8.7 Hz, 1H), 6.36 (s, 1H), 4.45 (t, *J* = 6.8 Hz, 2H), 4.07 (q, *J* = 7.0 Hz, 2H), 3.33 (t, *J* = 6.8 Hz, 2H), 1.44 (t, *J* = 7.0 Hz, 3H). ¹³C NMR (75 MHz, CDCl₃) δ 163.5, 158.2, 150.9, 149.3, 148.9, 144.1, 137.2, 136.4, 125.8, 125.1, 124.0, 121.7, 115.4, 114.6, 113.1, 111.4, 68.1, 64.8, 37.8, 14.7. ESI-MS *m/z*: 494.2 [M + H]⁺. HRMS (ESI) *m/z*: 493.9590 [M + H]⁺; Calcd for C₂₀H₁₇Br₂NO₄ (M + H) 493.9596.

5.1.4.8. (*Z*)-3,4-Dibromo-5-(3-ethoxy-4-(2-(5-ethylpyridin-2-yl)ethoxy)benzylidene) furan-2(5*H*)-one (**6k**). Yellow solid; yield 76.3%. ¹H NMR (300 MHz, CDCl₃) δ 8.39 (s, 1H), 7.47 (d, *J* = 7.5 Hz, 1H), 7.41 (d, *J* = 1.5 Hz, 1H), 7.30–7.27 (m, 2H), 6.92 (d, *J* = 8.4 Hz, 1H), 6.36 (s, 1H), 4.43 (t, *J* = 6.8 Hz, 2H), 4.07 (q, *J* = 7.0 Hz, 2H), 3.31 (t, *J* = 6.8 Hz, 2H), 2.64 (q, *J* = 7.6 Hz, 2H), 1.44 (t, *J* = 7.0 Hz, 3H), 1.24 (t, *J* = 7.6 Hz, 3H). ¹³C NMR (75 MHz, CDCl₃) δ 163.5, 155.3, 151.0, 148.9, 148.8, 144.1, 137.2, 136.9, 135.9, 125.8, 125.0, 123.7, 115.4, 114.6, 113.1, 111.4, 68.2, 64.8, 37.4, 25.7, 15.3, 14.7. ESI-MS *m/z*: 522.2 [M + H]⁺. HRMS (ESI) *m/z*: 521.9913 [M + H]⁺; Calcd for C₂₂H₂₁Br₂NO₄ (M + H) 521.9917.

5.1.4.9. (*Z*)-3,4-Dibromo-5-(3-ethoxy-4-(pyridin-2-ylmethoxy)benzylidene)furan-2(5*H*)-one (**6l**). Yellow solid; yield 83.4%. ¹H NMR (300 MHz, CDCl₃) δ 8.58 (d, *J* = 4.5 Hz, 1H), 7.71 (td, *J* = 7.8, 1.8 Hz, 1H), 7.56 (d, *J* = 7.8 Hz, 1H), 7.44 (d, *J* = 1.8 Hz, 1H), 7.26–7.17 (m, 2H), 6.90 (d, *J* = 8.4 Hz, 1H), 6.34 (s, 1H), 5.31 (s, 2H), 4.17 (q, *J* = 7.0 Hz, 2H), 1.50 (t, *J* = 7.0 Hz, 3H). ¹³C NMR (75 MHz, CDCl₃) δ 163.4, 156.81501, 149.0, 144.3, 137.2, 136.9, 125.5, 122.7, 121.1, 114.91, 114.4, 113.7, 111.6, 71.3, 64.7, 14.8. ESI-MS *m/z*: 480.3 [M + H]⁺. HRMS (ESI) *m/z*: 479.9417 [M + H]⁺; Calcd for C₁₉H₁₅Br₂NO₄ (M + H) 479.9447.

5.1.4.10. (*Z*)-3,4-Dibromo-5-(3-methoxy-4-(pyridin-2-ylmethoxy)benzylidene)furan-2(5*H*)-one (**6n**). Yellow solid; yield 80.8%. ¹H NMR (300 MHz, CDCl₃) δ 8.58 (d, *J* = 4.5 Hz, 1H), 7.70 (td, *J* = 7.7, 1.8 Hz, 1H), 7.52 (d, *J* = 7.7 Hz, 1H), 7.43 (d, *J* = 1.8 Hz, 1H), 7.25–7.16 (m, 2H), 6.90 (d, *J* = 8.4 Hz, 1H), 6.35 (s, 1H), 5.31 (s, 2H), 3.95 (s, 3H). ¹³C NMR (75 MHz, CDCl₃) δ 163.4, 156.6, 149.8, 149.6, 149.2, 144.3, 137.2, 136.9, 125.5, 125.5, 122.8, 121.3, 114.3, 113.3, 113.3, 111.7, 71.3,

56.1. ESI-MS *m/z*: 468.3 [M + H]⁺. HRMS (ESI) *m/z*: 465.9281 [M + H]⁺; Calcd for C₁₇H₁₁Br₂NO₃ (M + H) 465.9291.

5.1.4.11. (*Z*)-3,4-Dichloro-5-(4-(2-(5-ethylpyridin-2-yl)ethoxy)benzylidene)furan-2(5*H*)-one (**6p**). Yellow solid; yield 54.3%. ¹H NMR (300 MHz, CDCl₃) δ 8.40 (s, 1H), 7.73 (d, *J* = 9.0 Hz, 2H), 7.47 (d, *J* = 7.8 Hz, 1H), 7.19 (d, *J* = 7.8 Hz, 1H), 6.93 (d, *J* = 9.0 Hz, 2H), 6.34 (s, 1H), 4.40 (t, *J* = 6.7 Hz, 2H), 3.25 (t, *J* = 6.7 Hz, 2H), 2.64 (q, *J* = 7.6 Hz, 2H), 1.25 (t, *J* = 7.6 Hz, 3H). ¹³C NMR (75 MHz, CDCl₃) δ 162.5, 160.5, 155.1, 148.9, 142.6, 141.7, 137.3, 136.0, 132.9, 131.9, 124.4, 123.4, 115.2, 112.8, 67.4, 37.3, 25.7, 15.3. ESI-MS *m/z*: 390.4 [M + H]⁺. HRMS (ESI) *m/z*: 390.0639 [M + H]⁺; Calcd for C₂₀H₁₇Cl₂NO₃ (M + H) 390.0665.

5.1.4.12. (*Z*)-3,4-Dichloro-5-(4-(pyridin-2-ylmethoxy)benzylidene) furan-2(5*H*)-one (**6q**). Yellow solid; yield 71.0%. ¹H NMR (300 MHz, CDCl₃) δ 8.60 (d, *J* = 4.8 Hz, 1H), 7.76 (d, *J* = 8.9 Hz, 2H), 7.70 (m, 1H), 7.50 (d, *J* = 7.8 Hz, 1H), 7.25–7.21 (m, 1H), 7.02 (d, *J* = 8.9 Hz, 1H), 6.34 (s, 1H), 5.24 (s, 1H). ¹³C NMR (75 MHz, CDCl₃) δ 162.4, 159.9, 156.4, 149.3, 142.6, 141.9, 136.9, 133.0, 124.9, 122.8, 121.3, 118.2, 115.5, 112.5, 70.7. ESI-MS *m/z*: 348.1 [M + H]⁺. HRMS (ESI) *m/z*: 348.0181 [M + H]⁺; Calcd for C₁₇H₁₁Cl₂NO₃ (M + H) 348.0196.

5.1.4.13. (*Z*)-3,4-Dichloro-5-(3-ethoxy-4-(2-(pyridin-2-yl)ethoxy)benzylidene)furan-2(5*H*)-one (**6r**). Yellow solid; yield 76.3%. ¹H NMR (300 MHz, CDCl₃) δ 8.54 (d, *J* = 4.8 Hz, 1H), 7.62 (td, *J* = 7.5, 1.5 Hz, 1H), 7.39 (d, *J* = 1.8 Hz, 1H), 7.33 (d, *J* = 7.5 Hz, 1H), 7.29 (dd, *J* = 8.4, 1.8 Hz, 1H), 7.15 (dd, *J* = 4.8, 1.5 Hz, 1H), 6.92 (d, *J* = 8.4 Hz, 1H), 6.31 (s, 1H), 4.45 (t, *J* = 6.8 Hz, 2H), 4.06 (q, *J* = 7.0 Hz, 2H), 3.33 (t, *J* = 6.8 Hz, 2H), 1.43 (t, *J* = 7.0 Hz, 3H). ¹³C NMR (75 MHz, CDCl₃) δ 162.4, 158.2, 150.9, 149.3, 148.9, 142.6, 141.7, 136.3, 125.8, 124.8, 124.0, 121.6, 117.9, 115.4, 113.1, 113.1, 68.1, 64.8, 37.8, 14.7. ESI-MS *m/z*: 406.4 [M + H]⁺. HRMS (ESI) *m/z*: 406.0594 [M + H]⁺; Calcd for C₂₀H₁₇Cl₂NO₄ (M + H) 406.0614.

5.1.4.14. (*Z*)-3,4-Dichloro-5-(3-ethoxy-4-(pyridin-2-ylmethoxy)benzylidene)furan-2(5*H*)-one (**6s**). Yellow solid; yield 64.9%. ¹H NMR (300 MHz, CDCl₃) δ 8.61 (d, *J* = 4.5 Hz, 1H), 7.74 (td, *J* = 7.8, 1.8 Hz, 1H), 7.58 (d, *J* = 7.8 Hz, 1H), 7.47 (d, *J* = 1.8 Hz, 1H), 7.26–7.23 (m, 2H), 6.93 (d, *J* = 8.4 Hz, 1H), 6.34 (s, 1H), 5.34 (s, 2H), 4.20 (q, *J* = 7.0 Hz, 2H), 1.53 (t, *J* = 7.0 Hz, 3H). ¹³C NMR (75 MHz, CDCl₃) δ 162.3, 156.8, 150.2, 149.1, 142.6, 141.9, 136.9, 125.5, 125.3, 122.7, 121.1, 118.2, 114.9, 113.7, 112.9, 112.4, 71.3, 64.7, 14.7. ESI-MS *m/z*: 392.4 [M + H]⁺. HRMS (ESI) *m/z*: 392.0442 [M + H]⁺; Calcd for C₁₉H₁₅Cl₂NO₄ (M + H) 392.0458.

5.1.4.15. (*Z*)-3,4-Dichloro-5-(3-methoxy-4-(2-(pyridin-2-yl)ethoxy)benzylidene)furan-2(5*H*)-one (**6t**). Yellow solid; yield 79.9%. ¹H NMR (300 MHz, CDCl₃) δ 8.57 (d, *J* = 4.8 Hz, 1H), 7.65 (td, *J* = 7.7, 2.0 Hz, 1H), 7.40 (d, *J* = 2.1 Hz, 1H), 7.33 (d, *J* = 7.7 Hz, 1H), 7.30 (d, *J* = 8.7, 2.1 Hz, 1H), 7.22–7.15 (m, 1H), 6.95 (d, *J* = 8.7 Hz, 1H), 6.34 (s, 1H), 4.49 (t, *J* = 7.0 Hz, 2H), 3.90 (s, 3H), 3.37 (t, *J* = 7.0 Hz, 2H). ¹³C NMR (75 MHz, CDCl₃) δ 162.4, 157.9, 150.4, 149.5, 149.1, 142.6, 141.8, 136.7, 125.7, 124.8, 124.0, 121.8, 113.6, 113.0, 112.8, 112.6, 68.1, 56.1, 37.6. ESI-MS *m/z*: 392.3 [M + H]⁺. HRMS (ESI) *m/z*: 392.0456 [M + H]⁺; Calcd for C₁₉H₁₅Cl₂NO₄ (M + H) 392.0458.

5.1.4.16. (*Z*)-3,4-Dichloro-5-(3-methoxy-4-(pyridin-2-ylmethoxy)benzylidene)furan-2(5*H*)-one (**6u**). Yellow solid; yield 81.3%. ¹H NMR (300 MHz, CDCl₃) δ 8.61 (d, *J* = 4.5 Hz, 1H), 7.73 (td, *J* = 7.8, 1.8 Hz, 1H), 7.55 (d, *J* = 7.8 Hz, 1H), 7.45 (d, *J* = 1.8 Hz, 1H), 7.27 (d, *J* = 8.4, 1.8 Hz, 1H), 7.24 (d, *J* = 1.8 Hz, 1H), 6.93 (d, *J* = 8.4 Hz, 1H), 6.34 (s, 1H), 5.34 (s, 2H), 3.98 (s, 3H). ¹³C NMR (75 MHz, CDCl₃) δ 162.3, 156.5, 149.8, 149.6, 149.2, 142.6, 142.0, 136.9, 125.5, 125.2, 122.8, 121.3, 118.2, 113.4, 113.3, 112.8, 71.3, 56.1. ESI-MS *m/z*: 378.2

[M + H]⁺. HRMS (ESI) *m/z*: 378.0283 [M + H]⁺; Calcd for C₁₈H₁₃Cl₂NO₄ (M + H) 378.0302.

5.1.4.17. (*Z*)-3,4-Dibromo-5-(4-((3,5,6-trimethylpyrazin-2-yl)methoxy)benzylidene)furan-2(5*H*)-one (**6v**). Yellow solid; yield 82.0%. ¹H NMR (300 MHz, CDCl₃) δ 7.74 (d, *J* = 8.1 Hz, 1H), 7.03 (d, *J* = 8.1 Hz, 1H), 6.37 (s, 1H), 5.19 (s, 1H), 2.57 (s, 3H), 2.51 (s, 6H). ¹³C NMR (75 MHz, CDCl₃) δ 163.6, 160.2, 151.6, 149.9, 148.8, 145.1, 144.3, 137.2, 132.9, 125.1, 115.4, 114.1, 111.6, 69.9, 21.7, 21.4, 20.6. ESI-MS *m/z*: 481.5 [M + H]⁺. HRMS (ESI) *m/z*: 480.9585 [M + H]⁺; Calcd for C₁₉H₁₆Br₂N₂O₃ (M + H) 480.9587.

5.1.4.18. (*Z*)-3,4-Dibromo-5-(3-methoxy-4-((3,5,6-trimethylpyrazin-2-yl)methoxy)benzylidene)furan-2(5*H*)-one (**6w**). Yellow solid; yield 80.3%. ¹H NMR (300 MHz, CDCl₃) δ 7.36 (d, *J* = 2.1 Hz, 1H), 7.30 (dd, *J* = 8.4, 2.1 Hz, 1H), 7.08 (d, *J* = 8.4 Hz, 1H), 6.33 (s, 1H), 5.26 (s, 2H), 3.89 (s, 1H), 2.61 (s, 1H), 2.51 (s, 6H). ¹³C NMR (75 MHz, CDCl₃) δ 162.3, 151.4, 150.1, 150.1, 149.8, 148.6, 145.1, 142.6, 141.9, 125.4, 125.2, 118.2, 113.7, 113.6, 112.9, 70.8, 56.0, 21.7, 21.4, 20.7. ESI-MS *m/z*: 511.3 [M + H]⁺. HRMS (ESI) *m/z*: 510.9734 [M + H]⁺; Calcd for C₂₀H₁₈Br₂N₂O₄ (M + H) 510.9693.

5.1.5. General procedure for synthesis of 2-(bromomethyl)-3,5,6-trimethylpyrazine (**C₃**)

Compound **C₃** was prepared according to a published method [51].

5.1.6. General procedures for synthesis of **B₂C₃**

To a solution of benzaldehyde derivatives (**B₂**, 1.0 mmol) in dry DMF (30 mL) was added potassium carbonate (K₂CO₃, 2.0 mmol) and **C₃** (1.2 mmol). And the mixture was stirred for 10 h at 85 °C, then it was cooled to room temperature. The reaction mixture was filtered, washed with water and the filtrate was extracted with CH₂Cl₂. The organic layer was dried over Na₂SO₄ overnight and evaporated to give a residue which was chromatographed using ethyl acetate/petroleum ether (1:6, v/v) to get the intermediate products **B₂C₃**.

5.1.6.1. 4-((3,5,6-Trimethylpyrazin-2-yl)methoxy)benzaldehyde. White solid; yield 81.1%. ¹H NMR (300 MHz, CDCl₃) δ 9.89 (s, 1H), 7.83 (d, *J* = 8.7 Hz, 2H), 7.12 (d, *J* = 8.7 Hz, 2H), 5.24 (s, 2H), 2.59 (s, 3H), 2.53 (s, 6H). ¹³C NMR (75 MHz, CDCl₃) δ 190.8, 163.5, 151.8, 150.0, 148.8, 144.8, 132.0, 130.3, 115.2, 70.1, 21.7, 21.4, 20.6. ESI-MS *m/z*: 257.3 [M + H]⁺.

5.1.6.2. 3-Methoxy-4-((3,5,6-trimethylpyrazin-2-yl)methoxy)benzaldehyde. White solid; yield 76.3%. ¹H NMR (300 MHz, CDCl₃) δ 9.85 (s, 1H), 7.45 (d, *J* = 1.8 Hz, 1H), 7.42 (s, 1H), 7.18 (d, *J* = 1.8 Hz, 1H), 5.31 (s, 2H), 3.91 (s, 3H), 2.62 (s, 3H), 2.52 (s, 6H). ¹³C NMR (75 MHz, CDCl₃) δ 190.9, 153.5, 151.5, 150.2, 150.1, 148.7, 144.9, 130.5, 126.5, 112.7, 109.4, 70.8, 56.0, 21.6, 21.3, 20.6. ESI-MS *m/z*: 287.3 [M + H]⁺.

5.1.6.3. 3-Ethoxy-4-((3,5,6-trimethylpyrazin-2-yl)methoxy)benzaldehyde. White solid; yield 81.3%. ¹H NMR (300 MHz, CDCl₃) δ 9.84 (s, 1H), 7.43 (d, *J* = 1.8 Hz, 1H), 7.40 (s, 1H), 7.18 (d, *J* = 1.8 Hz, 1H), 5.31 (s, 2H), 4.14 (q, *J* = 7.0 Hz, 2H), 2.64 (s, 3H), 2.53 (s, 6H), 1.45 (t, *J* = 7.0 Hz, 3H). ¹³C NMR (75 MHz, CDCl₃) δ 190.9, 153.6, 151.4, 150.2, 149.6, 148.5, 145.1, 130.6, 126.2, 113.2, 110.8, 71.0, 64.5, 21.7, 21.3, 20.7, 14.6. ESI-MS *m/z*: 301.2 [M + H]⁺.

5.1.6.4. 3-((3,5,6-Trimethylpyrazin-2-yl)methoxy)benzaldehyde. White solid; yield 75.4%. ¹H NMR (300 MHz, CDCl₃) δ 9.65 (s, 1H), 7.27 (s, 1H), 7.15 (d, *J* = 1.8 Hz, 1H), 7.13 (d, *J* = 1.8 Hz, 1H), 7.00 (dd, *J* = 1.8, 1.8 Hz, 1H), 4.94 (s, 2H), 2.32 (s, 3H), 2.22 (s, 6H). ¹³C NMR (300 MHz, CDCl₃) δ 191.4, 158.9, 151.1, 149.6, 148.4, 144.9, 137.6,

129.9, 123.2, 121.5, 113.4, 69.8, 21.4, 21.1, 20.3. ESI-MS *m/z*: 257.3 [M + H]⁺.

5.1.7. General procedures for synthesis of **7a–7d**

To compound thiazolidinedione (**A₂**, 1.2 mmol) in toluene (40 mL) was added **B₂C₃** (1.0 mmol), and the reaction mixture was stirred under the atmosphere of nitrogen. Then a catalytic amount of 2-methyl piperidine and glacial acetic acid were added dropwise to the solution over a period of 10 min, heated at 130 °C for 2 h. A lot of solid would precipitate out when the solution cooled to room temperature. At last, the reaction mixture was filtered and washed with toluene and saturated salt water to get products **7a–7d**.

5.1.7.1. (*Z*)-5-(4-((3,5,6-Trimethylpyrazin-2-yl)methoxy)benzylidene)thiazolidine-2,4-dione (**7a**). White solid; yield 81.5%. ¹H NMR (300 MHz, DMSO-*d*₆) δ 7.73 (s, 1H), 7.56 (d, *J* = 8.9 Hz, 2H), 7.19 (d, *J* = 8.9 Hz, 2H), 5.23 (s, 2H), 2.48 (s, 3H), 2.45 (d, 6H). ¹³C NMR (75 MHz, DMSO-*d*₆) δ 168.6, 168.3, 160.4, 151.6, 149.7, 148.8, 145.3, 132.4, 131.8, 126.4, 121.4, 116.0, 69.9, 21.7, 21.4, 20.5. ESI-MS *m/z*: 356.3 [M + H]⁺. HRMS (ESI) *m/z*: 356.1066 [M + H]⁺; Calcd for C₁₈H₁₇N₃O₃S (M + H) 356.1071.

5.1.7.2. (*Z*)-5-(3-Methoxy-4-((3,5,6-trimethylpyrazin-2-yl)methoxy)benzylidene)thiazolidine-2,4-dione (**7b**). White solid; yield 89.6%. ¹H NMR (300 MHz, DMSO-*d*₆) δ 7.71 (s, 1H), 7.27 (d, *J* = 8.4 Hz, 1H), 7.20 (d, *J* = 1.9 Hz, 1H), 7.16 (dd, *J* = 8.4, 1.9 Hz, 1H), 5.20 (s, 2H), 3.79 (s, 3H), 2.48 (s, 3H), 2.45 (s, 3H), 2.44 (s, 3H). ¹³C NMR (75 MHz, DMSO-*d*₆) δ 168.9, 168.9, 151.6, 150.0, 149.9, 149.7, 148.8, 145.4, 131.8, 126.9, 123.8, 122.1, 114.2, 113.9, 70.4, 56.0, 21.7, 21.4, 20.5. ESI-MS *m/z*: 386.3 [M + H]⁺. HRMS (ESI) *m/z*: 386.1165 [M + H]⁺; Calcd for C₁₉H₁₉N₃O₄S (M + H) 386.1176.

5.1.7.3. (*Z*)-5-(3-Ethoxy-4-((3,5,6-trimethylpyrazin-2-yl)methoxy)benzylidene)thiazolidine-2,4-dione (**7c**). White solid; yield 88.7%. ¹H NMR (300 MHz, DMSO-*d*₆) δ 7.78 (s, 1H), 7.24 (d, *J* = 8.7 Hz, 1H), 7.19 (d, *J* = 1.8 Hz, 1H), 7.13 (dd, *J* = 8.7, 1.8 Hz, 1H), 5.21 (s, 2H), 4.06 (q, *J* = 6.9 Hz, 2H), 2.49 (s, 3H), 2.46 (s, 3H), 2.45 (s, 3H), 1.31 (t, *J* = 6.9 Hz, 3H). ¹³C NMR (75 MHz, DMSO-*d*₆) δ 168.4, 168.2, 151.5, 150.1, 149.6, 149.0, 148.6, 145.6, 129.3, 128.7, 127.8, 125.81, 123.4, 114.8, 71.0, 64.4, 21.7, 21.4, 20.6, 15.0. ESI-MS *m/z*: 400.4 [M + H]⁺. HRMS (ESI) *m/z*: 398.1183 [M – H][–]; Calcd for C₂₀H₁₇Br₂NO₄ (M – H) 398.1172.

5.1.7.4. (*Z*)-5-(3-((3,5,6-Trimethylpyrazin-2-yl)methoxy)benzylidene)thiazolidine-2,4-dione (**7d**). White solid; yield 81.8%. ¹H NMR (300 MHz, DMSO-*d*₆) δ 7.70 (s, 1H), 7.44 (t, *J* = 8.1 Hz, 1H), 7.25–7.09 (m, 3H), 5.21 (s, 2H), 2.49 (s, 3H), 2.45 (s, 6H). ¹³C NMR (75 MHz, DMSO-*d*₆) δ 169.0, 168.9, 159.1, 151.5, 149.7, 148.7, 145.6, 135.1, 131.2, 130.8, 125.5, 123.0, 117.4, 116.1, 69.9, 21.6, 21.4, 20.6. ESI-MS *m/z*: 356.3 [M + H]⁺. HRMS (ESI) *m/z*: 354.0914 [M – H][–]; Calcd for C₂₀H₁₇Br₂NO₄ (M – H) 354.0910.

5.2. Biological assays and experimental procedures

5.2.1. Cell culture

RAW264.7 murine macrophages were cultured in DMEM containing 10% new-born calf serum, 100 units/mL penicillin, and 100 μg/mL streptomycin at 37 °C in a 5% CO₂ humidified atmosphere.

5.2.2. Assay for NO production

RAW264.7 cells were inoculated at 5 × 10⁴ cells per well in 96-well plate and cultured for 18 h. The cells were then pre-treated with 10 μM compounds which were prepared in serum-free medium for 2 h before stimulation with LPS (100 ng/mL). After

stimulated for 48 h by LPS, the NO produced in the culture medium was quantified by Griess reagent, in brief, added 100 μ L of Griess reagent (1% sulfanilamide and 0.1% N-(1-naphthyl)ethylenediamine dihydrochloride in 5% phosphoric acid) to 100 μ L of supernatant medium and incubated for 10 min at room temperature, then measured absorbance of the samples at 540 nm (OD_{540}) in a microplate reader (Bio-Rad Laboratories, CA, USA). Rosiglitazone and indomethacin were used as positive controls. NO inhibition rate = $[\text{control } (OD_{540}) - \text{compound } (OD_{540})] / [\text{control } (OD_{540}) - \text{blank } (OD_{540})] \times 100\%$.

Control: treated with LPS only.

Compound: treated with LPS and compounds.

Blank: cultured with fresh medium only.

5.2.3. Cell cytotoxicity

Cell cytotoxicity was evaluated by methyl thiazolyl tetrazolium (MTT) assay. RAW264.7 cells were inoculated at 4×10^3 cells per well in 96-well plate. After cultured for 16 h, the cells were treated with different compounds which were diluted in DMEM for 48 h. Then 20 μ L of 0.5 mg/mL MTT reagent was added into the cells and incubated for 4 h. After 4 h, cell culture was removed and then 150 μ L DMSO was added to dissolve the formazan. The optical density was measured at 570 nm (OD_{570}). Cell viability was calculated from three independent experiments. The density of formazan formed in blank group was set as 100% of viability. Cell viability (%) = $\text{compound } (OD_{570}) / \text{blank } (OD_{570}) \times 100\%$

Blank: cultured with fresh medium only.

Compound: treated with compounds or LPS.

5.2.4. Measurement of TNF- α and IL-6

RAW264.7 cells (5×10^5 cells/well) were cultured in 24-well plate and pretreated with 10 μ M of compounds for 2 h, and then LPS was added. The production of TNF- α and IL-6 was stimulated by the addition of 100 ng/mL LPS and incubated for 6 h, 12 h and 24 h. The levels of TNF- α and IL-6 in the supernatant were determined using the mouse ELISA kit (TNF- α : MultiSciences, EK2822; IL-6: MultiSciences, EK2062) which is operated according to the manufacturer's instructions.

5.2.5. Western blot analysis

RAW264.7 cells were seeded into a 6-well culture plate at a density of 2×10^6 cells per well, and then cultured for 18 h. Then, the culture medium was replaced by fresh medium containing 10 μ M compounds, and 500 ng/mL LPS was added. After cultured for another 4 h, the cells were harvested and lysed with IP buffer (Beyotime, P0013) supplemented with 1 mM phenylmethanesulfonyl fluoride (PMSF; Beyotime, ST506) for 30 min at 4 $^{\circ}$ C. The cell lysates were centrifuged at $14,000 \times g$ for 10 min at 4 $^{\circ}$ C to remove insoluble materials and the supernatant was collected. Total protein concentration was determined using a BCA protein assay kit (Thermo Scientific, 23227). Each protein sample was mixed with a quarter volume of 5X SDS-PAGE sample loading buffer (100 mmol/L Tris-HCl pH 6.8, 4% SDS, 5% β -mercaptoethanol, 20% glycerol, and 0.1% bromophenol blue) and boiled for 10 min. Equal amounts of total cellular protein were loaded per well in 12.5% precast SDS-PAGE gels and then transferred to polyvinylidene difluoride membranes (Bio-Rad) for over 60 min at 300 mA. The membranes were blocked with 5% non-fat dry milk in TBS plus 0.1% Tween 20 (TBST) for 2 h at room temperature, washed 3 times in TBST for 5 min each, incubated with the primary antibody (anti-phosphorylation of SAPK/JNK (Thr183/Tyr185), anti-SAPK/JNK, anti-phosphorylation of ERK1/2 (Thr202/Tyr204), anti-ERK1/2, anti-phosphorylation of p38 (Thr180/Tyr182), anti-p38, anti-phosphorylation of I κ B α (Ser32/36), anti-I κ B α , anti-phosphorylation of NF- κ B p65, and anti-NF- κ B p65) at 4 $^{\circ}$ C

overnight (all the primary antibodies were purchased from Cell Signaling Technology and diluted in TBST at the ratio of 1:1000), washed 3 times in TBST for 5 min each, incubated with anti-rabbit or anti-mouse secondary antibody (1:1000 in TBST, Cell Signaling Technology) for 90 min, washed in TBST and exposed to ECL reagents.

5.2.6. Molecular modeling

First, using the Sketch Molecule module in SYBYL 8.1 program package of Tripos, the minimized energy structures of four ligands were built by using the standard Tripos molecular mechanics force field and Gasteiger-Hückel charge [52,53]. The structure of PPAR γ was obtained from the Protein Data Bank (PDB ID: 2PRG), all ligands and water molecules were removed and the polar hydrogen atoms were added. The docking calculation was performed using the empirical scoring function and the patented search engine in Surflex-Dock. The Molecular Computer Aided Design (MOLCAD) program was employed to display cavity depth potential or hydrogen bonds of the PPAR γ binding site within the four compounds.

Acknowledgment

This work was supported by the National Natural Science Foundation of China (81072554).

Appendix A. Supplementary data

These data include MOL files and InChIKeys of the most important compounds described in this article.

References

- [1] R. Medzhitov, *Cell* 140 (2010) 771–776.
- [2] C.C. Corriveau, R.L. Danner, *Infect. Agents Dis.* 2 (1993) 35–43.
- [3] H. Baumann, J. Gauldie, *Immunol. Today* 15 (1994) 74–80.
- [4] T. Lawrence, D.A. Willoughby, D.W. Gilroy, *Nat. Rev. Immunol.* 2 (2002) 787–795.
- [5] P. Kubes, D.M. McCafferty, *Am. J. Med.* 109 (2000) 150–158.
- [6] H.Y. Park, G.Y. Kim, J.W. Hyun, H.J. Hwang, N.D. Kim, B.W. Kim, Y.H. Choi, *Int. J. Mol. Med.* 29 (2012) 1146–1152.
- [7] J.M. Micking, Q.W. Xie, C. Nathan, *Annu. Rev. Immunol.* 15 (1997) 323–350.
- [8] G. Pascual, A.L. Fong, S. Ogawa, A. Gamliel, A.C. Li, V. Perissi, D.W. Rose, T.M. Willson, M.G. Rosenfeld, C.K. Glass, *Nature* 437 (2005) 759–763.
- [9] R. Kostadinova, W. Wahli, L. Michalik, *Curr. Med. Chem.* 12 (2005) 2995–3009.
- [10] A.L. Hevener, J.M. Olefsky, D. Reichart, G. Bandyopadhyay, C. Benner, M.A. Febbraio, et al., *J. Clin. Invest.* 117 (2007) 1658–1669.
- [11] M. Hasegawa-Moriyama, T. Kurimoto, M. Nakama, K. Godai, M. Kojima, T. Kuwaki, Y. Kanmura, *Biochem. Biophys. Res. Commun.* 426 (2012) 76–82.
- [12] C. Jiang, A.T. Ting, B. Seed, *Nature* 391 (1998) 82–86.
- [13] N. Liu, J.T. Liu, Y.Y. Ji, P.P. Lu, J. Cardiovasc. Pharmacol. 57 (2011) 348–356.
- [14] A. Jahoor, R. Patel, A. Bryan, C. Do, J. Krier, C. Watters, W. Wahli, G. Li, S.C. Williams, K.P. Rumbaugh, *J. Bacteriol.* 190 (2008) 4408–4415.
- [15] W.T. Wu, C.C. Lee, C.J. Lee, Y.M. Subeq, R.P. Lee, B.G. Hsu, *Biol. Res. Nurs.* 13 (2011) 38–43.
- [16] J.S. Hwang, E.S. Kang, S.A. Ham, T. Yoo, H. Lee, K.S. Paek, C. Park, J.H. Kim, D.S. Lim, H.G. Seo, *Mediators Inflammation* 352807 (2012) 1–9.
- [17] Z.S. Buss, Y.S. Medeiros, T.S. Frode, *Inflammation* 35 (2012) 280–288.
- [18] J.L. Guo, B.Z. Li, W.M. Chen, P.H. Sun, Y.Q. Wang, *Lett. Drug Des. Discovery* 6 (2009) 107–113.
- [19] P.H. Sun, Z.Q. Yang, M.K. Li, W.M. Chen, Q. Liu, X.S. Yao, *Lett. Drug Des. Discovery* 6 (2009) 568–574.
- [20] Y.T. Wang, W.M. Chen, A.X. Hu, R.W. Jiang, G. Cao, W.K. Su, D. Guan, *J. Struct. Chem.* 28 (2009) 191–194.
- [21] X.Y. Li, J.L. He, H.T. Liu, W.M. Li, C. Yu, J. Ethnopharmacol. 125 (2009) 83–89.
- [22] Y.M. Sue, C.F. Cheng, C.C. Chang, Y. Chou, C.H. Chen, S.H. Juan, *Nephrol. Dial. Transplant.* 24 (2009) 769–777.
- [23] F. Bellina, R. Rossi, *Synthesis* 12 (2007) 1887–1889.
- [24] G.Y. Liu, B.Q. Guo, W.N. Chen, C. Cheng, Q.L. Zhang, M.B. Dai, J.R. Sun, P.H. Sun, W.M. Chen, *Chem. Biol. Drug Des.* 79 (2012) 628–638.
- [25] Y. Wu, S. Karna, C.H. Choi, M. Tong, H.H. Tai, D.H. Na, C.H. Jang, H. Cho, *J. Med. Chem.* 54 (2011) 5260–5264.
- [26] W.F. Annette, B. Franz, *Lett. Org. Chem.* 10 (2013) 2–7.
- [27] J.P. Uttaro, S. Broussous, C. Mathe, C. Perigaud, *Tetrahedron* 69 (2013) 2131–2136.

- [28] M. Ren, J. Dong, Y.G. Xu, N. Wen, G.Q. Gong, *Chem. Biodiversity* 7 (2010) 2727–2736.
- [29] P. Rajakumar, M.G. Swaroop, S. Jayavelu, K. Murugesan, *Tetrahedron* 62 (2006) 12041–12050.
- [30] G. Bruno, L. Costantino, C. Curinga, R. Maccari, F. Monforte, F. Nicolo, R. Ottana, M.G. Vigorita, *Bioorg. Med. Chem.* 10 (2002) 1077–1084.
- [31] Z. Xu, C. Knaak, J. Ma, Z.M. Beharry, C. McInnes, W. Wang, A.S. Kraft, C.D. Smith, *J. Med. Chem.* 52 (2009) 74–86.
- [32] A. Kar, S. Gogoi, N.P. Argade, *Tetrahedron* 61 (2005) 5297–5302.
- [33] L.C.A. Barbosa, C.R.A. Maltha, A.J. Demuner, P.F. Pinheiro, J.O.S. Varejao, R.M. Montanari, N.J. Andrade, *Quim. Nova* 33 (2010) 2020–2026.
- [34] P. Vallance, *Fundam. Clin. Pharmacol.* 17 (2003) 1–10.
- [35] C.A. Dinarello, *Chest* 118 (2000) 503–508.
- [36] B. Kaminska, *Biochim. Biophys. Acta* 1754 (2005) 253–262.
- [37] A. Salminen, J. Huuskonen, J. Ojala, A. Kauppinen, K. Kaarniranta, T. Suuronen, *Ageing. Res. Rev.* 7 (2008) 83–105.
- [38] P.J. Barnes, M. Karin, *N. Engl. J. Med.* 336 (1997) 1066–1071.
- [39] R.J. Ulevitch, P.S. Tobias, *Annu. Rev. Immunol.* 13 (1995) 437–457.
- [40] H.Y. Pyo, I. Jou, S.Y. Jung, S. Hong, E.H. Joe, *Neuroreport* 9 (1998) 871–874.
- [41] Y.P. Bai, Y.H. Liu, J. Chen, T. Song, Y. You, Z.Y. Tang, Y.J. Li, G.G. Zhang, *Biochem. Biophys. Res. Commun.* 360 (2007) 20–26.
- [42] Z.J. Chen, J. Hagler, V.J. Palombella, F. Melandri, D. Scherer, D. Ballard, T. Maniatis, *Genes. Dev.* 9 (1995) 1586–1597.
- [43] M. Karin, Y. Ben-Neriah, *Annu. Rev. Immunol.* 18 (2000) 621–663.
- [44] J. Baldwin, S. Albert, *Annu. Rev. Immunol.* 14 (1996) 649–683.
- [45] G. Pearson, F. Robinson, T.B. Gibson, B.E. Xu, M. Karandikar, K. Berman, M.H. Cobb, *Endocr. Rev.* 22 (2001) 153–183.
- [46] K. Matter, M.S. Balda, *Nat. Rev. Mol. Cell. Biol.* 4 (2003) 225–237.
- [47] D. Chen, R.J. Davis, R.A. Flavell, *Annu. Rev. Immunol.* 20 (2002) 55–72.
- [48] L.M. Leesnitzer, D.J. Parks, R.K. Bledsoe, J.E. Cobb, J.L. Collins, T.G. Consler, R.G. Davis, E.A. Hull-Ryde, J.M. Lenhard, L. Patel, et al., *Biochemistry* 41 (2002) 6640–6650.
- [49] Sybyl 8.1. Tripos Inc.; St. Louis, MO, USA, 2008.
- [50] B. Bohman, L. Jeffares, G. Flematti, L.T. Byrne, B.W. Skelton, R.D. Phillips, K.W. Dixon, R. Peakall, R.A. Barrow, *J. Nat. Prod.* 75 (2012) 1589–1594.
- [51] P.L. Wang, G.M. She, Y.N. Yang, Q. Li, H.G. Zhang, J. Liu, Y.Q. Cao, X. Xu, H.M. Lei, *Molecules* 17 (2012) 4972–4985.
- [52] P. Lan, J.R. Sun, W.N. Chen, P.H. Sun, W.M. Chen, *J. Enzyme Inhib. Med. Chem.* 26 (2011) 367–377.
- [53] J. Gasteiger, M. Marsili, *Tetrahedron* 36 (1980) 3219–3228.